

Dynamic Impact Analysis of Bagless Transfer System 3013 Can in Drops at Various Inclination Angles

by

C. Gong

Westinghouse Savannah River Company
Savannah River Site
Aiken, South Carolina 29808

D. R. Leduc

BEST AVAILABLE COPY
For Entire Document

A document prepared for 2001 ASME PRESSURE VESSELS AND PIPING CONFERENCE at Atlanta, GA, USA
from 7/22/2001 - 7/26/2001.

DOE Contract No. **DE-AC09-96SR18500**

This paper was prepared in connection with work done under the above contract number with the U. S. Department of Energy. By acceptance of this paper, the publisher and/or recipient acknowledges the U. S. Government's right to retain a nonexclusive, royalty-free license in and to any copyright covering this paper, along with the right to reproduce and to authorize others to reproduce all or part of the copyrighted paper.

RECORDS ADMINISTRATION



R0290027

This document was prepared in conjunction with work accomplished under Contract No. DE-AC09-96SR18500 with the U.S. Department of Energy.

DISCLAIMER

This report was prepared as an account of work sponsored by an agency of the United States Government. Neither the United States Government nor any agency thereof, nor any of their employees, makes any warranty, express or implied, or assumes any legal liability or responsibility for the accuracy, completeness, or usefulness of any information, apparatus, product or process disclosed, or represents that its use would not infringe privately owned rights. Reference herein to any specific commercial product, process or service by trade name, trademark, manufacturer, or otherwise does not necessarily constitute or imply its endorsement, recommendation, or favoring by the United States Government or any agency thereof. The views and opinions of authors expressed herein do not necessarily state or reflect those of the United States Government or any agency thereof.

This report has been reproduced directly from the best available copy.

Available for sale to the public, in paper, from: U.S. Department of Commerce, National Technical Information Service, 5285 Port Royal Road, Springfield, VA 22161, phone: (800) 553-6847, fax: (703) 605-6900, email: orders@ntis.fedworld.gov online ordering: <http://www.ntis.gov/ordering.htm>

Available electronically at <http://www.doe.gov/bridge>

Available for a processing fee to U.S. Department of Energy and its contractors, in paper, from: U.S. Department of Energy, Office of Scientific and Technical Information, P.O. Box 62, Oak Ridge, TN 37831-0062, phone: (865) 576-8401, fax: (865) 576-5728, email: reports@adonis.osti.gov

DYNAMIC IMPACT ANALYSIS OF BAGLESS TRANSFER SYSTEM 3013 CAN IN DROPS AT VARIOUS INCLINATION ANGLES

*Chung Gong, Daniel R. Leduc
Savannah River Technology Center
Westinghouse Savannah River Company
773-42A, Room 154
Aiken, South Carolina 29808-0001*

Telephone: (803) 725-3167, Fax: (803) 725-8829, e-mail: chung.gong@srs.gov

ABSTRACT

The purpose of this analysis is to provide rational judgment for the most pernicious impact angle of dropping. A numerical simulation method, finite element analysis, is adopted for this study. The general-purpose finite element analysis code, ABAQUS® [HKS, 1998], facilitates the numerical computation. The geometrical finite element modeling is developed with the software PATRAN® [MSC, 1999]. The finite element code ABAQUS® has been verified according to the QA plans.

MATHEMATICAL MODELING

The severity of the damage to the 3013 vessel from a free fall drop is a function of many parameters, the obvious factors in the modeling are:

1. geometrical configuration;
2. material properties of the vessel;
3. contents in the vessel;
4. the configuration and distribution of the mass of the contents;
5. height of drop;
6. orientation of the drop
7. when the vessel reaches the unyielding ground, the region of contact on the vessel;
8. finite elements selected; and
9. the time integration method applied.

The Hanford Bagless Transfer System (BTS) 3013 vessel is a truncated bagless transfer can, which is the inner can of the 3013 configuration. The top and bottom ends are considerably different as shown in Figure 1. This figure also demonstrates the finite element mesh.

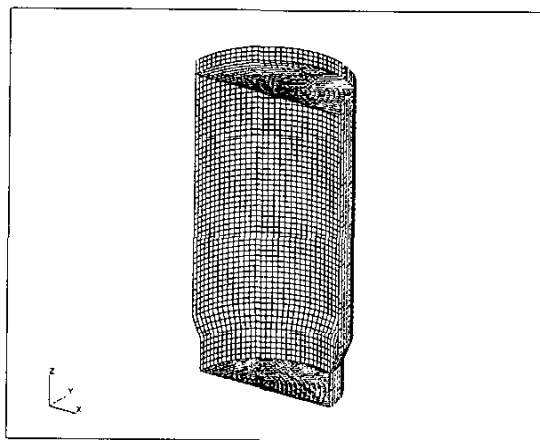


Figure 1. Finite Element Mesh of the Bagless 3013 Vessel

Without the impact of secondary rebounding drop, the free fall drop of the vessel at any orientation possesses a plane of symmetry involving the vertical axis of the vessel, provided that the mass in the vessel is uniformly distributed. Since the contents in the vessel are uncertain and irregular in configuration, the materials inside the vessel cannot be accurately modeled. Particularly in the dynamic analysis, the movement of the interior materials will have significant impact on the extent of damage to the vessel. In order to demonstrate the physical effects of the enclosed interior mass, two mathematical models are developed:

1. The 5 kg mass of the interior material is uniformly distributed over the entire finite element mesh of the 3013 vessel;
2. A solid steel cylinder of 3 inches in diameter and 5.5156 inches in height is inserted inside the 3013 vessel. The steel cylinder is free to move inside the vessel during the impact. The weight of the steel cylinder is 5 kg.

The 3013 vessel is composed of stainless steel type 304L. The mechanical properties of the 304L stainless steel can be found in [Sindelar, 1993]. The interior material has a mass of 5 kg. The height

of the vessel is 9-inch and the outer diameter 4.6-inch. The bottom end is tapered off to a diameter of 4.1-inch. The thickness of the cylinder is 0.06-inch. The top lid is 0.12-inch thick, whereas the bottom of the vessel is 0.25-inch thick.

The mechanical properties of the stainless steel and the steel cylindrical mass are listed in the table:

Table 1. Mechanical Properties of the Stainless Steel and the Carbon Steel.

	<i>Stainless Steel Type 304L</i>	<i>Carbon Steel</i>
Modulus of Elasticity (psi)	28.30E+06	30.00E+06
Poisson's Ratio	0.30	0.30
Mass Density $\left(\frac{\text{pounds} \cdot \text{second}^2}{\text{inch}^4}\right)$	7.324E-04	7.324E-04

In the case when the included mass of 5-kg is uniformly distributed over the bagless 3013 vessel, the equivalent mass density of the vessel is $2.872825\text{E-}03$ [(lbf-sec²)/in⁴]. The included cylindrical mass remains in elastic state through dynamic impact process (for conservatism). However, the bagless 3013 vessel is elasto-plastic with strain hardening. The stress-strain curve of stainless steel type 304L at room temperature is plotted in Figure 2.

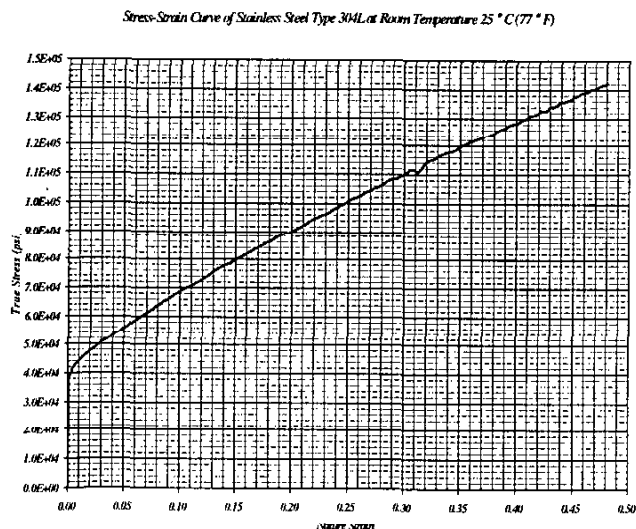


Figure 2. The Stress-Strain Curve of Stainless Steel Type 304L

The whole package will drop from 30-foot and 8-foot elevations to flat unyielding surface at all possible orientations.

The 3013 vessel is modeled with shell elements (4009 nodes, 3918 elements). The cylindrical mass is modeled with 3D continuum elements (5539 nodes, 4704 elements). The total number of nodes is 9548 and the total number of elements is 8622. Explicit integration method is applied to the solution of the dynamic equations.

Since the top and bottom configurations of the 3013 vessel are different, drop simulations in both directions are considered.

The dynamic impact computation starts at the moment as a corner of the vessel touches the rigid surface. In the case of uniformly distributed mass the center of mass is fixed for both top and bottom drops.

Whereas, in the case of a movable cylindrical mass inside the vessel, the mass center varies as the point of contact during drop changes.

The initial velocities for the 30-foot and 8-foot drops are computed as follows:

$$V_{30-foot} = \sqrt{2gh} = \sqrt{2 \times 386.04 \times 30 \times 12} = 527.2085 \text{ inches / second} \quad (1)$$

$$V_{8-foot} = \sqrt{2gh} = \sqrt{2 \times 386.04 \times 8 \times 12} = 272.2493 \text{ inches / second} \quad (2)$$

Let θ be the angle of inclined drop of the vessel. The angle is measured from the vertical axis. Then velocity components in the vertical (V_z) and horizontal (V_x) directions are:

$$V_{z(30-foot)} = V_{30-foot} \cos(\theta) \quad (3)$$

$$V_{x(30-foot)} = V_{30-foot} \sin(\theta)$$

$$V_{z(8-foot)} = V_{8-foot} \cos(\theta) \quad (4)$$

$$V_{x(8-foot)} = V_{8-foot} \sin(\theta)$$

The steel cylindrical mass is free to move inside the bagless 3013 vessel during the impact process. Nevertheless, in this analysis, the initial position of the cylindrical mass inside the vessel is specified in each orientation of drop. The end edge of the cylinder is located at the corner of the vessel, which is in contact with the rigid surface at the moment when the bagless 3013 vessel touches the ground from the drop. The initial positions of the cylindrical mass for top and bottom drops are shown in Figures 3 and 4 respectively.

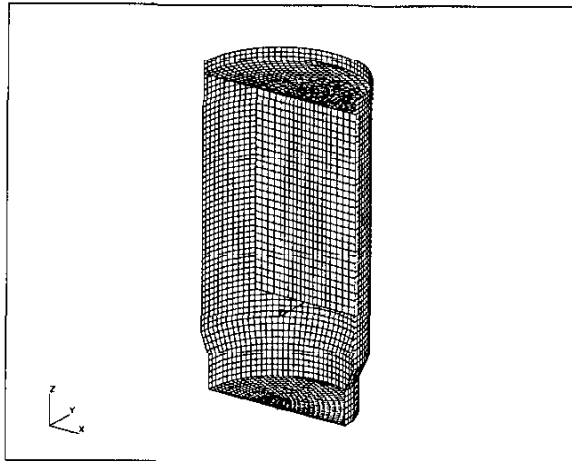


Figure 3. The initial position of the Steel Cylindrical Mass inside the Bagless 3013 Vessel for Inclined Top Drops

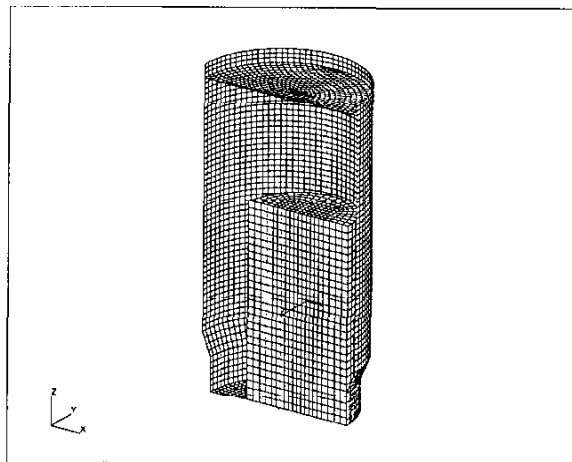


Figure 4. The initial position of the Steel Cylindrical Mass inside the Bagless 3013 Vessel for Inclined Bottom Drops

The location and distribution of the included 5-kg mass inside the vessel shift the center of mass (or gravity) of the bagless 3013 system.

Table 2. The Center of Mass (or Gravity) of the Bagless 3013 System.

Location or Distribution of the included 5-kg Mass	CENTER OF MASS		
	X (inches)	Y (inches)	Z (inches)
Uniformly Distributed over the Vessel	0.0	0.0	4.133172
Cylindrical Mass at the Top Right Corner	0.5956140	0.0	5.424185
Cylindrical Mass at the Bottom Right Corner	0.4094847	0.0	3.109184

The drop of a package with a sharp corner in contact with a rigid surface will certainly generate plastic deformation in the area of impact. The severity of the damage is a function of:

1. Angle of inclination when the vessel hits the rigid surface;
2. Position and distribution of the included mass inside the vessel;
3. The geometric configuration and stiffness distribution of the vessel;
4. The material properties (particularly in the plastic range) of the vessel and the included mass inside vessel; and
5. The height of drop.

The analyses indicate that the most severe damage to the area of impact occurs in the neighborhood of a particular inclined drop angle. The inclination angle that forms with the vertical axis (Z-axis in this analysis) and the line joining the center of mass (or gravity) and the corner point, which will first touch the rigid surface during the drop. This angle of mass center over point of impact varies with the mass distribution in the vessel as well as the direction (top drop or bottom drop) of the drop. The angle of mass center over point of impact for the four types of combined mass distributions and drop directions are listed in the table:

Table 3. The Angle of Mass Center over Point of Impact

Location or Distribution of the included 5-kg Mass	The Angle of Mass Center Over Point Of Impact With respect to the vertical axis (degrees)
Uniformly Distributed over the Vessel, Top Drop	25.2948
Uniformly Distributed over the Vessel, Bottom Drop	26.3808
Cylindrical Mass at the Top Right Corner	25.4845
Cylindrical Mass at the Bottom Right Corner	27.8177

RESULTS

The location and severity of impact damage in the vessel from a drop are a function of many factors as explained previously. The distribution

and positions of the included mass are certainly important factors. The four mass distributions and positions selected in this study are very practical and realistic for the drop tests proposed. Under these conditions, the dynamic impact may inflict the worst damage to the vessel during a drop.

Without any knowledge of the contents in the vessel, an assumption of uniform distribution of the mass over the entire vessel skin is a practical solution. In the 8-foot drop tests, a steel cylindrical mass is encased inside the vessel. The cylindrical mass is free to move (both translation and rotation in all directions) inside the vessel. The initial relative position of the cylindrical mass inside the vessel will significantly influence the damage severity of the vessel in a particular drop orientation. If intuitive perception can serve as guidance, as the vessel is positioned for drop at a certain angle, the cylindrical mass inside the vessel would slide to the lowest corner by gravity. These are the initial positions of the cylindrical mass as shown in Figures 3 and 4.

The cylindrical mass at the vessel corner will provide double impact (impact from outside rigid surface and impact from the corner of the cylindrical mass) to the elements at the area of contact. Likewise, the cylindrical mass absorbs a sizeable amount of energy at the initial impact and reduces the kinetic energy that would propagate into the vessel. If the cylindrical mass were attached to a location other than the lowest corner in the vessel, the dynamic impact consequence would be very different during the drop process. The initially high kinetic energy would mostly dissipated through plastic deformation in the vessel itself and the cylindrical mass would deliver a second blow upon the vessel. Hence, the four kinematic conditions suggested earlier might be the most realistic and the most detrimental to the vessel with the test circumstances provided.

The results from these four analyses provide an abundant insight understanding of the mechanics on the dynamic impact process in an elasto-plastic medium.

In the theory of metal plasticity the von Mises yield criterion is a function of von Mises equivalent stress. The plastic strain is expressed in terms of the so-called equivalent plastic strain, which is defined as:

$$\epsilon^{pl} = \bar{\epsilon}^{pl} \quad \text{or} \quad \sqrt{\frac{2}{3} d\epsilon_{ij}^{pl} d\epsilon_{ij}^{pl}}. \quad (5)$$

Where, $\bar{\epsilon}^{pl}$ is the initial equivalent plastic strain, and $d\epsilon_{ij}^{pl}$ is the ij -component of plastic strain rate. In the rate independent plasticity, the equivalent plastic strain can be put in the form:

$$\epsilon^{pl} = \sqrt{\frac{2}{3} \epsilon_{ij}^{pl} \epsilon_{ij}^{pl}} \quad (6)$$

In metal plasticity, the plastic volumetric deformation is zero.

Consequently, the plastic strain component ϵ_{ij}^{pl} , in essence, can be replaced with the deviatoric plastic strain component, viz.,

$$\epsilon_{ij}^{pl} = \epsilon_{ij}^{pl} - \frac{1}{3} \epsilon_{kk}^{pl} \delta_{ij}. \quad (7)$$

Thus the equivalent plastic strain in metal plasticity has the form:

$$\epsilon^{pl} = \sqrt{\frac{2}{3} \epsilon_{ij}^{pl} \epsilon_{ij}^{pl}}. \quad (8)$$

A. The Vessel With Uniformly Distributed Mass Drops From 30-Foot on The Top

The mass of the vessel is heavier than conventional stainless steel due to the additional 5-kg material distributed over the entire vessel. However, the strength of the steel remains the same. The kinetic energy $[0.5 * \text{mass} * (\text{velocity})^2]$ is increased. The energy dissipated, in this analysis, will all be plastic energy in the deformed vessel.

The maximum von Mises equivalent stress and the maximum equivalent plastic strain in the vessel during each drop is listed as follows:

Table 4. The Maximum von Mises Equivalent Stress and the Maximum Equivalent Plastic Strain in the Vessel During Each Drop

Drop Angle with respect to the vertical Vessel Axis	Comments	Maximum Plastic Strain	In Element	Maximum von Mises Equivalent Stress	In Element	at Time
Degrees			(Layer)	psi	(Layer)	milliseconds
0.0	Vertical Top Down	0.1480	3532 (5)	78902	3532 (5)	0.5000
20	Inclined Top Down	0.3760	3420 (1)	124360	3420 (1)	2.4000
25.2948	Aligned with Mass Center, Top Down	0.4186	3420 (1)	132110	3420 (1)	2.0000
30	Inclined Top Down	0.4507	3420 (1)	134480	3419 (1)	2.1000
32	Inclined Top Down	0.4549	3420 (1)	136730	3419 (1)	2.0000
35	Inclined Top Down	0.4499	3420 (1)	134320	3417 (1)	2.1000
45	Inclined Top Down	0.4081	3419 (1)	129810	3419 (1)	1.6500
26.3808	Aligned with Mass Center Bottom Down	0.3508	841 (5)	119940	841 (5)	2.7500

The ultimate tensile strain of the 304L stainless steel is 40%. It implies that in those locations the equivalent plastic strains accumulated above 40% material fracture could be developed. The maximum strains are shown at the elements at the junction of the thick vessel lid and the thin cylindrical wall. At 32-degree with respect to the vertical axis of the vessel, the equivalent plastic strain reaches the maximum value of 45.49%. The angle of 32-degree probably is the angle of drop inflicts worst damage to the vessel. The equivalent plastic strain in each drop is plotted against the orientation of drops in Figure 5.

3013 Vessel with Uniformly Distributed Mass (5-kg) Plotted with respect to the Angles of Vertical Up side down (Top) Drop from 30-foot

The maximum equivalent plastic strain is an essential indicator of the severity of traumatizing in a structural system during a dynamic impact. In the 30-foot top drop, the equivalent plastic strain reaches a maximum value of 0.4549 (45.49%) that is above the ultimate strain 40%. The highest equivalent plastic strain is in the element that connecting the thick lip and thinner cylinder wall. The inclination angle for this maximum strain is 32° from the vertical axis.

The transaction of energies in the vessel system during the dynamic impact is an important vehicle to the understanding of the mechanical behavior of the vessel. The time history of the energy fluctuation during each of the inclined drops is plotted. The vessel has little recoverable elastic strain energy in each of the drops. Most of the kinetic energy is dissipated through plastic deformation.

B. The Vessel With Uniformly Distributed Mass Drops From 30-Foot on The Bottom

As discussed previously, the inclination angle of drop for maximum damage is in the neighborhood of the angle that aligns the center of mass with the point of impact contact. A bottom drop analysis with the mass center over the contact point shows the results:

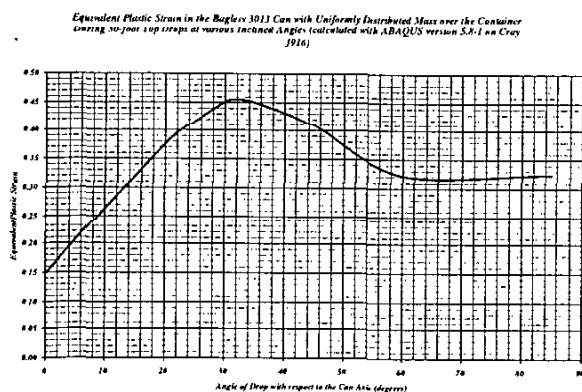


Figure 5. Maximum Equivalent Plastic Strain in the

Table 5. The Maximum von Mises Equivalent Stress and the Maximum Equivalent Plastic Strain in the Vessel During the Drop.

<i>Drop Angle with respect to the vertical Vessel Axis</i>	<i>Comments</i>	<i>Maximum Plastic Strain</i>	<i>In Element</i>	<i>Maximum von Mises Equivalent Stress</i>	<i>In Element</i>	<i>at Time</i>
<i>Degrees</i>			<i>(Layer)</i>	<i>psi</i>	<i>(Layer)</i>	<i>milliseconds</i>
26.5808	Aligned with Mass Center, Bottom Down	0.3508	841 (5)	119940	841 (5)	2.75

At the bottom neck area where the vessel begins to change diameter, the vessel has large deformation. The shell is folding and stress is high. This area without a solid cylinder inside absorbs most of the initial kinetic energy. The time history of the energies is shown at the end of this paper.

C. The Vessel With a Steel Cylindrical Mass Drops From 30-Foot on The Top

With a free-moving solid cylindrical mass (5-kg) inside, the vessel will experience multiple dynamic impact. Depends upon the initial position of the included cylindrical mass, the vessel may have double impact at the point of first contact to the rigid surface. If the cylindrical mass is not at point of initial impact, the cylindrical mass may smash into the vessel in a already deformed region, then the damage could be more serious.

The dynamic effect of the free-moving cylindrical mass inside the vessel can be perceived in the plot of the maximum equivalent plastic strain in the vessel, as shown in Figure 5. The maximum plastic strains in the vessel with free-moving cylindrical mass are much higher than that in the vessel with uniformly distributed mass. The maximum equivalent plastic strain in the vessel with uniformly distributed mass is

45.49% at the inclined drop angle of 32°, whereas in the vessel with solid cylindrical mass inside, the maximum equivalent plastic strain escalates up to 76.04% at the angle of 20°. The plastic strain is well above the ultimate strain (40%) of the stainless steel (type 304L).

The non-uniformity of the vessel thickness and configuration influence the wave propagation in the vessel. However, the most pronounced dynamic effect is the free moving cylindrical mass inside the vessel. The mass center of the cylindrical mass is apart from the mass center of the vessel and even the mass center of the whole system. Consequently, the impact force transmitted through the vessel contact surface to the cylindrical mass inside will induce translation and rotation motion in addition to elastic deformation in the cylindrical mass. The motion of the cylindrical mass changes the severity of damage upon the vessel during dynamic impact. This result implies that the configuration, mass density, mechanical properties and the initial position of the included mass inside the vessel during dynamic impact can significantly impinge on the damage scenarios of the vessel.

The maximum equivalent plastic strain and von Mises equivalent stress for each drop condition are listed in the following table.

Table 6. The Maximum von Mises Equivalent Stress and the Maximum Equivalent Plastic Strain in the Vessel During Each Drop

Drop Angle with respect to the vertical Vessel Axis Degrees	Comments	Maximum Plastic Strain	In Element	Maximum von Mises Equivalent Stress	In Element	at Time
			(Layer)	psi	(Layer)	milliseconds
0	Vertical Top Down	0.341	3536 (5)	109540	3535 (1)	1.8
10	Inclined Top Down	0.5832	3536 (5)	142220	3534 (5)	0.75
20	Inclined Top Down	0.7604	3583 (1)	142220	3581 (1)	0.85
21	Inclined Top Down	0.7515	3583 (1)	142220	3526 (1)	0.75
25.48446	Aligned with Mass Center, Top Down	0.6854	3583 (1)	142220	3530 (1)	0.65
30	Inclined Top Down	0.6005	3532 (1)	142220	3530 (1)	0.7
40	Inclined Top Down	0.6558	3536 (5)	142220	3536 (5)	0.6
50	Inclined Top Down	0.4786	3536 (5)	141160	3536 (5)	0.75
60	Inclined Top Down	0.6142	3536 (5)	142220	3536 (5)	0.6
70	Inclined Top Down	0.5986	3536 (5)	142220	3534 (5)	0.85
80	Inclined Top Down	0.5694	3536 (5)	142220	3534 (5)	0.85

The maximum equivalent plastic strains for the top drops from 30-foot for the vessel with a steel cylindrical mass inside are plotted in Figure 6.

Equivalent Plastic Strain in the Bagless 3013 Can with Steel Cylindrical Mass Inside During 30-foot Top Drops at various Inclined Angles with respect to the Vertical Vessel Axis (calculated with ABAQUS version 5.8.1 on Cray T3E)

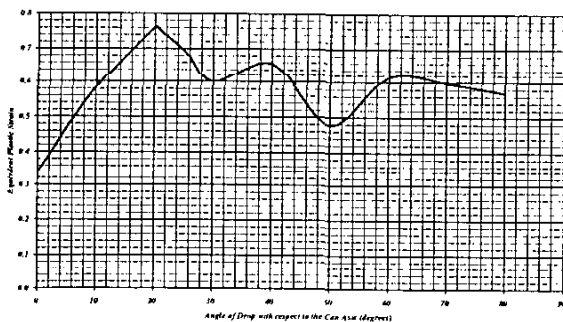


Figure 6. Maximum Equivalent Plastic Strain in the 3013 Vessel with a Steel Cylindrical Mass (5-kg) inside the Vessel Plotted with respect to the Angles of Vertical Up side down (Top) Drop from 30-foot

The time histories of the kinetic, plastic and elastic strain energies during the dynamic impact process will be saved at the end of this paper.

D. The Vessel With a Steel Cylindrical Mass Drops From 8-Foot on The Top

Based upon the concept of linear analysis, the curve of maximum equivalent plastic strain with respect to the inclined drop angles for the 8-foot drop should have the same pattern as that for the 30-foot drop. However, in reality, both geometrical and material nonlinearities in the vessel and the free moving cylindrical mass inside completely modify the pattern of the curve of maximum equivalent plastic strain. The maximum equivalent plastic strain and the maximum von Mises equivalent stress for each drop angle are listed in the table.

Table 7. The Maximum von Mises Equivalent Stress and the Maximum Equivalent Plastic Strain in the Vessel During Each Drop

Drop Angle with respect to the vertical Vessel Axis	Comments	Maximum Plastic Strain	In Element	Maximum von Mises Equivalent Stress	In Element	at Time
Degrees			(Layer)	psi	(Layer)	milliseconds
0	Vertical Top Down	0.157	3533 (1)	80808	3533 (1)	0.55
10	Inclined Top Down	0.3242	3536 (1)	115150	3536 (1)	1.55
20	Inclined Top Down	0.3927	3532 (1)	127580	3532 (1)	1.45
25.4845	Aligned with Mass Center, Top Down	0.4411	3536 (1)	135460	3534 (1)	1.55
26	Inclined Top Down	0.4397	3534 (1)	135630	3534 (1)	1.6
30	Inclined Top Down	0.4255	3534 (1)	132880	3534 (1)	1.55
40	Inclined Top Down	0.373	3534 (1)	122410	3536 (1)	1.5
50	Inclined Top Down	0.3816	3536 (5)	125380	3536 (5)	1.2
60	Inclined Top Down	0.3453	3534 (1)	117530	3532 (1)	1.55
70	Inclined Top Down	0.3309	3534 (1)	116330	3534 (1)	1.45
80	Inclined Top Down	0.3105	3536 (1)	111370	3534 (1)	1.7

The maximum equivalent plastic strain has a maximum at 25.4845° that is the angle when the mass center of the vessel and the cylindrical mass is aligned with the corner of contact to the rigid surface initially during the drop.

The motion of the cylindrical mass inside the vessel still causes fluctuation in the maximum equivalent plastic strain as the inclination angle increases. However, the magnitude of variation is much smaller as compared with that of the 30-foot drop. In the 30-foot drops, the peak of the maximum equivalent plastic strain of each of the mass distributions (uniform distribution over the vessel and a solid cylindrical mass inside the vessel) occurs away from the special angle at which the mass center of the vessel (and the included mass) is aligned with the initial point of impact during the drop.

In the case of uniformly distributed mass over the vessel, the shift of the peak of the maximum equivalent plastic strain is mostly due to the material properties of the stainless steel. The ultimate strength of the stainless steel type 304L is 142,216 psi (true stress) (or 87,945 psi, engineering stress). In the numerical modeling (as well as physically possible), when the kinetic energy (in this analysis) in the vessel stresses certain elements in the vessel to the limit of ultimate strength, the residual energy will deform the vessel much further without increasing the stress level.

With a solid cylindrical mass inside the vessel, the motion and deformation of the cylinder will significantly affect the deformation of the vessel itself. The energy plots for the 30-foot drops show that the elastic strain energy in the cylindrical mass has a substantial effect on the history of the kinetic energy in the vessel. Whereas for the 8-foot drops, the elastic strain energy in the cylindrical mass is negligibly small. Consequently the existence of the cylindrical mass in the vessel has little influence on the peak of the maximum equivalent plastic strain as a function of inclination of drop. The time histories of energies are saved at the end of this paper.

The maximum equivalent plastic strain as a function of the angle of drop from 8-foot is plotted in Figure 7.

Equivalent Plastic Strain in the Begless 3013 Can with Steel Cylindrical Mass inside During 8-foot Top Drops at various Inclined Angles with respect to the Vertical Vessel Axis (calculated with ABAQUS version 5.8.1 on Cray J916)

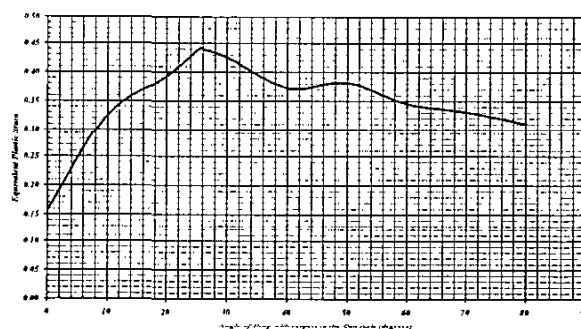


Figure 7. Maximum Equivalent Plastic Strain in the 3013 Vessel with a Steel Cylindrical Mass (5-kg) inside the Vessel Plotted with respect to the Angles of Vertical Up side down (Top) Drop from 8-foot

E. The Vessel With a Steel Cylindrical Mass Drops From 8-Foot on The Bottom

By arranging the initial position of the cylindrical mass inside the vessel at the bottom corner of first impact point, the dynamic consequence upon the vessel has two major effects.

1. Since the edge of the cylindrical mass is directly at the point of impact, the cylinder rebounds immediately as the vessel touches the rigid surface. The subsequent motion of the cylindrical mass will influence the deformation history of the vessel.

2. The cylinder at the point of impact absorbs a sizable amount of energy and stores as elastic strain energy in the mass. Initially the kinetic energy transmitting to the vessel is significantly reduced.

In the top drop case, the scenario is different. The 0.375-inch lip at the top of the vessel will absorb most part of the energy from initial blow of dynamic impact. The residual kinetic energy is minuscule in the case of 8-foot drop, such that the cylindrical mass has little deformation and movement during the dynamic impact process. Whereas in the case of 30-foot drop, the residual energy in the vessel after heavily deformed the lip, still so powerful that when transmitted to the cylindrical mass, the residual power deforms the cylindrical mass.

These physical phenomena of complicated dynamic interaction and wave propagations are fully divulged in the time histories of energies.

The maximum equivalent plastic strains and the maximum von Mises equivalent stresses for the bottom drops of the vessel with a steel cylinder inside are listed in the following table.

The maximum equivalent plastic strain in the vessel varies with the inclination angle of drop. The peak of the plastic strain is at the angle 27.8177-degree that is the angle when the center of mass is aligned with the bottom corner of the vessel. The maximum equivalent plastic strain at that angle is 18.18%, which is well below the ultimate strain (40%). The curve of the plastic strain is plotted in Figure 8.

Table 8. The Maximum von Mises Equivalent Stress and the Maximum Equivalent Plastic Strain in the Vessel During Each Drop

Drop Angle with respect to the vertical Vessel Axis	Comments	Maximum Plastic Strain	In Element	Maximum von Mises Equivalent Stress	In Element	at Time
Degrees			(Layer)	psi	(Layer)	milliseconds
0	Vertical Bottom Down	0.032833	3916 (1)	52157	3916 (1)	2.10
10	Vertical Bottom Down	0.094392	470 (5)	66853	470 (5)	0.10
20	Vertical Bottom Down	0.1518	567 (5)	79007	567 (5)	0.25
27.8177	Aligned with Mass Center Bottom Down	0.1818	567 (5)	86699	567 (5)	0.45
30	Vertical Bottom Down	0.1791	567 (5)	86098	567 (5)	0.45
40	Vertical Bottom Down	0.1674	567 (5)	83569	567 (5)	0.25
50	Vertical Bottom Down	0.1344	471 (1)	46084	335 (5)	0.25
60	Vertical Bottom Down	0.098782	567 (5)	67296	567 (5)	1.95
70	Vertical Bottom Down	0.091846	519 (5)	66045	519 (5)	0.10
80	Vertical Bottom Down	0.1166	2309 (5)	72414	2309 (5)	2.50

Equivalent Plastic Strain in the Bagless 3013 Can with Steel Cylindrical Mass Inside During 8-foot Bottom Drop at various Inclined Angles with respect to the Vertical Vessel Axis (this calculation is performed with ABAQUS version 5.8.19, No shock)

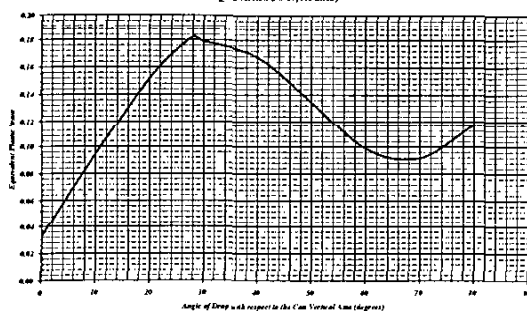


Figure 8. Maximum Equivalent Plastic Strain in the 3013 Vessel with a Steel Cylindrical Mass (5-kg) inside the Vessel Plotted with respect to the Angles of Vertical Bottom down Drop from 8-foot

CONCLUSION

For the bagless transfer 3013 vessel with included 5-kg mass of any configuration, determining the worst angle of drops is a difficult question, because all the geometrical configurations and material properties of the vessel and the included mass have decisive influence upon the drop results. The mechanical behavior of this dynamic impact is highly nonlinear that involves both geometrical and material nonlinearities.

The major factors that influence the drop results:

1. Mechanical properties of the materials (both bagless 3013 vessel and the cylindrical mass):
 - i. Moduli of elasticity
 - ii. Poisson's ratios
 - iii. Yield strength
 - iv. Ultimate strength
 - v. Stress-strain curve (full range of the material strengths)
2. Geometrical configuration of the vessel and the cylindrical mass
3. Distribution of the mass inside the vessel

4. The height of drop that determines the initial kinetic energy in the system
5. The relative position of the cylindrical mass inside the vessel
6. Orientation of the drop
7. Types of Finite Elements selected in the analysis:
 - i. Solid continuum element
 - ii. Structural shell elements
8. Method of solution
 - i. implicit integration
 - ii. explicit integration

Due to computational limitations, this analysis takes advantage of both solid continuum elements (included cylindrical mass) and structural shell elements (bagless transfer 3013 vessel). The dynamic impact

analysis adopts the explicit integration method that saves both computer memory and CPU time.

In the case of 30-foot drop, the drop angle for maximum equivalent plastic strain, which is an important parameter in determining the severity of damage, is away from the angle that aligns the center of mass with the point of initial impact in the drop. The difference in the mass distribution and the motion of the included cylindrical mass cause the deviation.

In the 8-foot drops, both top and bottom drops, the peaks of maximum equivalent plastic strain are at the angle that the center of mass is aligned with the point of initial impact. The motion of the cylindrical mass inside has little effect on the angle for the most severe damage to the vessel.

The results for the four cases are listed in the following table:

Table 9. The Final Results.

Cases	Drop angle aligned center of mass with the point of initial impact (degrees)	Angle of peak maximum equivalent plastic strain (degrees)	Maximum equivalent plastic strain (%)	Maximum equivalent von Mises stress (psi)
30-foot top-drop, Included 5-kg mass uniformly distributed over the vessel	25.2948	32	45.49	136,730
30-foot top-drop, a steel cylindrical mass (5-kg) inside the vessel	25.4845	20	76.04	142,220
8-foot top drop, a steel cylindrical mass (5-kg) inside the vessel	25.4845	25.4845	44.11	135,460
8-foot bottom drop, a steel cylindrical mass (5-kg) inside the vessel	27.8177	27.8177	18.18	86,699

For 8-foot drops the drop angle with the center of mass aligned with the point of initial impact is the inclination angle, which will induce the worst impact damage.

The contour fringe drawings of the equivalent plastic strain and the von Mises equivalent stress are shown at the end of this paper. The contour fringe drawings are produced for all the drops and inclination angles. However, only the above four cases and the 30-foot bottom drop with uniformly distributed mass are included.

REFERENCES

HKS, 1998, *ABAQUS Theory manual, ABAQUS / Explicit User's Manual*, versions 5.8-1 and 5.8-19, Hibbitt, Karlsson & Sorensen, Inc., 1080 Main Street, Pawtucket, RI 02860-4847, Telephone: 401-727-4200.

MSC, 1999, *MSC / PATRAN*, version 8.5, The MacNeal-Schwendler Corporation, 815 Colorado Boulevard, Los Angeles, Telephone: 213-258-9111.

Sindelar, R. L., 1993, *Tensile Properties of Type 304 / 304L Stainless Steel for Impact Deformation Analysis of Nuclear Materials Containers (U)*, SRT-MTS-93-3113, November 10, 1993.

Time History of Kinetic, Plastic and Elastic Strain Energies in the Bagless 3013 Can with Uniformly Distributed Mass over the Container During the Vertical Top Drop from 30-foot

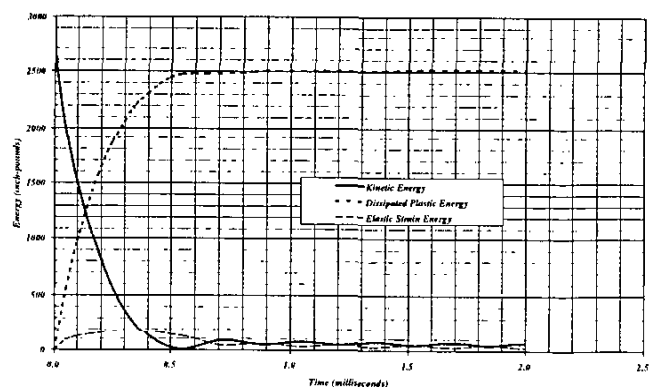


Figure 9. Time History of Kinetic, Plastic and Elastic Strain Energies during the Vertical Top Drop from 30-foot

Time History of Kinetic, Plastic and Elastic Strain Energies in the Bagless 3013 Can with Uniformly Distributed Mass over the Container During the 20-degree Inclined Top Drop from 30-foot

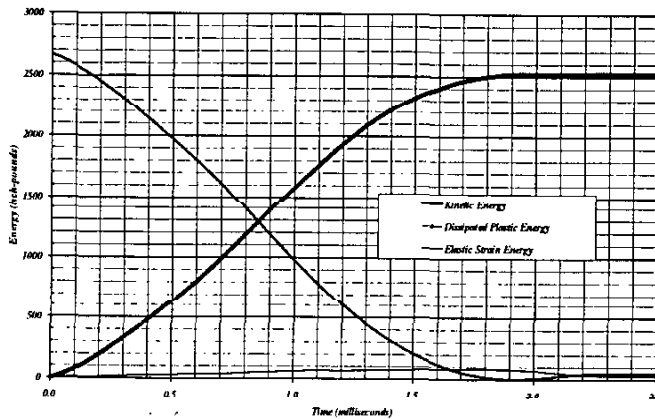


Figure 10. Time History of Kinetic, Plastic and Elastic Strain Energies during the 20-degree Inclined Top Drop from 30-foot

Time History of Kinetic, Plastic and Elastic Strain Energies in the Bagless 3013 Can with Uniformly Distributed Mass over the Container During the (25.2948-degree) Inclined Top Drop Aligned with Mass Center from 30-foot

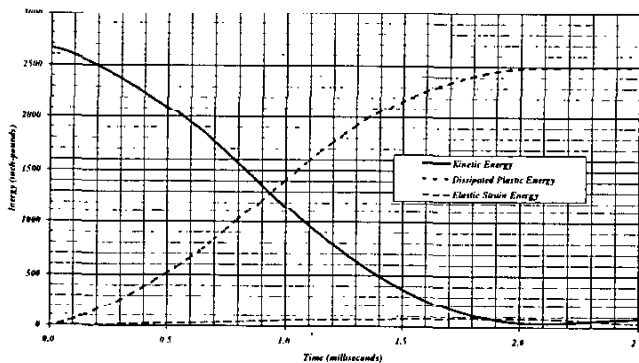


Figure 11. Time History of Kinetic, Plastic and Elastic Strain Energies during the 25.2948-degree Inclined Top Drop Aligned with Mass Center from 30-foot

Time History of Kinetic, Plastic and Elastic Strain Energies in the Bagless 3013 Can with Uniformly Distributed Mass over the Container During the 30-degree Inclined Top Drop from 30-foot

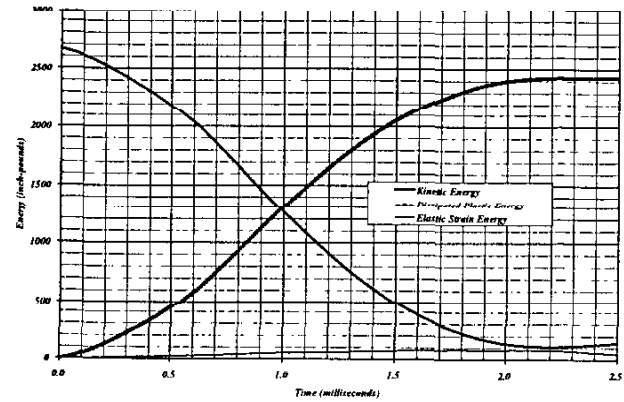


Figure 12. Time History of Kinetic, Plastic and Elastic Strain Energies during the 30-degree Inclined Top Drop from 30-foot

Time History of Kinetic, Plastic and Elastic Strain Energies in the Bagless 3013 Can with Uniformly Distributed Mass over the Container During the 32-degree Inclined Top Drop from 30-foot

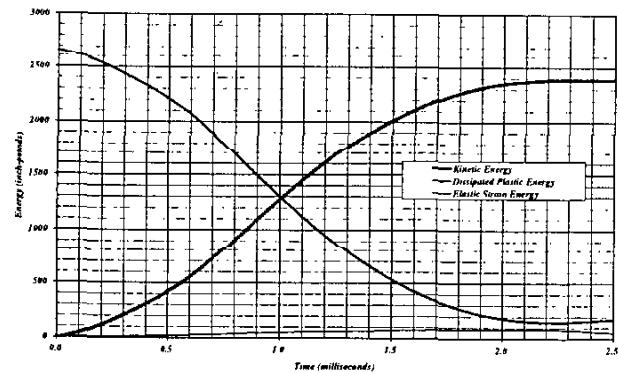


Figure 13. Time History of Kinetic, Plastic and Elastic Strain Energies during the 32-degree Inclined Top Drop from 30-foot

Time History of Kinetic, Plastic and Elastic Strain Energies in the Bagless 3013 Can with Uniformly Distributed Mass over the Container During the 35-degree Inclined Top Drop from 30-foot

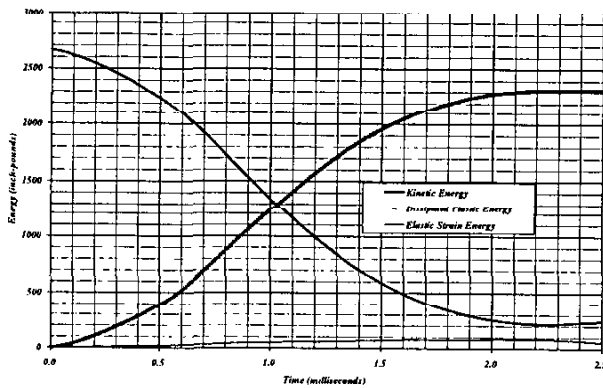


Figure 14. Time History of Kinetic, Plastic and Elastic Strain Energies during the 35-degree Inclined Top Drop from 30-foot

Time History of Kinetic, Plastic and Elastic Strain Energies in the Bagless 3013 Can with Uniformly Distributed Mass over the Container During the 60-degree Inclined Top Drop from 30-foot

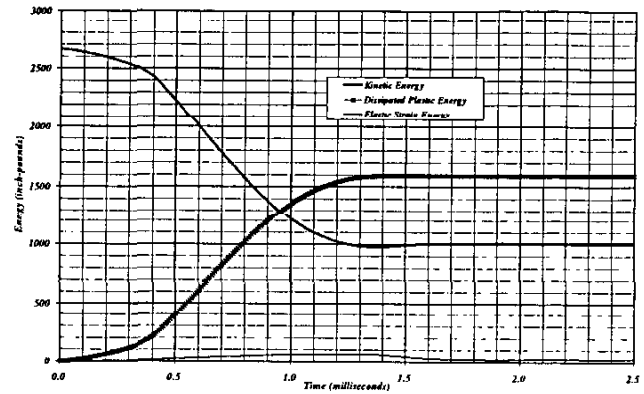


Figure 16. Time History of Kinetic, Plastic and Elastic Strain Energies during the 60-degree Inclined Top Drop from 30-foot

Time History of Kinetic, Plastic and Elastic Strain Energies in the Bagless 3013 Can with Uniformly Distributed Mass over the Container During the 45-degree Inclined Top Drop from 30-foot

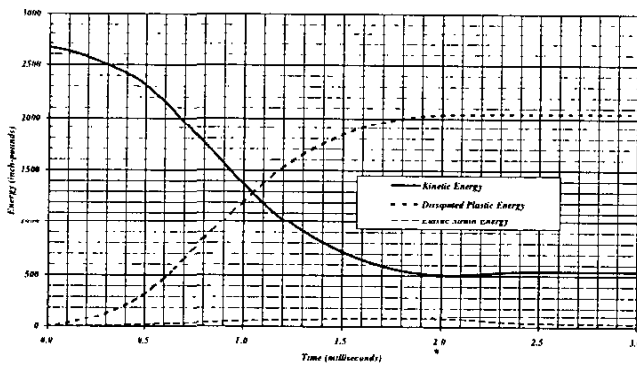


Figure 15. Time History of Kinetic, Plastic and Elastic Strain Energies during the 45-degree Inclined Top Drop from 30-foot

Time History of Kinetic, Plastic and Elastic Strain Energies in the Bagless 3013 Can with Uniformly Distributed Mass over the Container During the 85-degree Inclined Top Drop from 30-foot

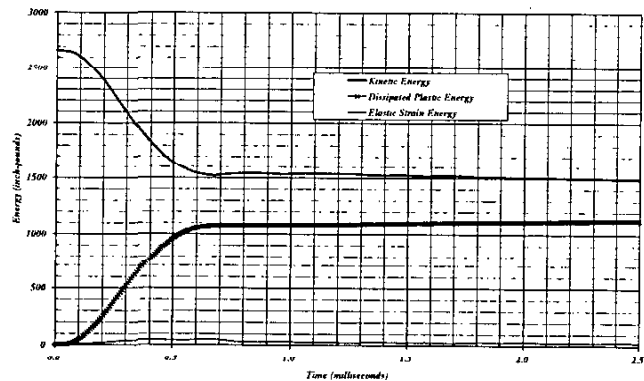


Figure 17. Time History of Kinetic, Plastic and Elastic Strain Energies during the 85-degree Inclined Top Drop from 30-foot

Time History of Kinetic, Plastic and Elastic Strain Energies in the Bagless 3013 Can with Uniformly Distributed Mass over the Container During the 26.3808-degree Inclined Bottom Drop Aligned with Mass Center from 30-foot

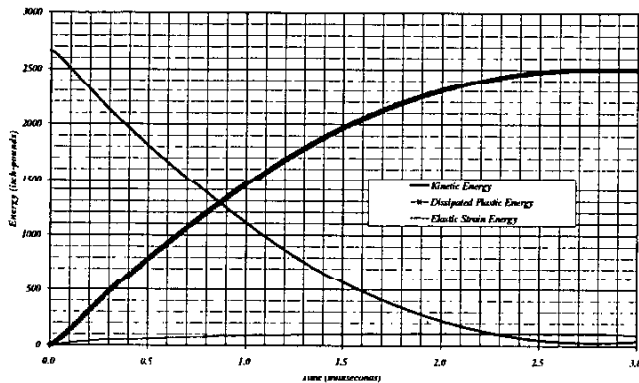


Figure 18. Time History of Kinetic, Plastic and Elastic Strain Energies during the 26.3808-degree Inclined Bottom Drop Aligned with Mass Center from 30-foot

Time History of Kinetic, Plastic and Elastic Strain Energies in the Bagless 3013 Can with a Steel Cylindrical Mass inside During the Upside Down Top Drop from 30-foot (calculated with ABAQUS version 5.8.1 on Cray J916)

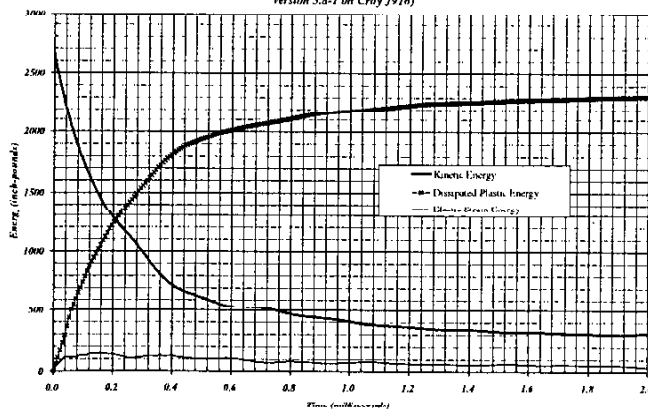


Figure 19. Time History of Kinetic, Plastic and Elastic Strain Energies during the Upside Down Top Drop from 30-foot

Time History of Kinetic, Plastic and Elastic Strain Energies in the Bagless 3013 Can with a Steel Cylindrical Mass inside During the 10-degree Inclined Upside Down Top Drop from 30-foot (calculated with ABAQUS version 5.8.1 on Cray J916)

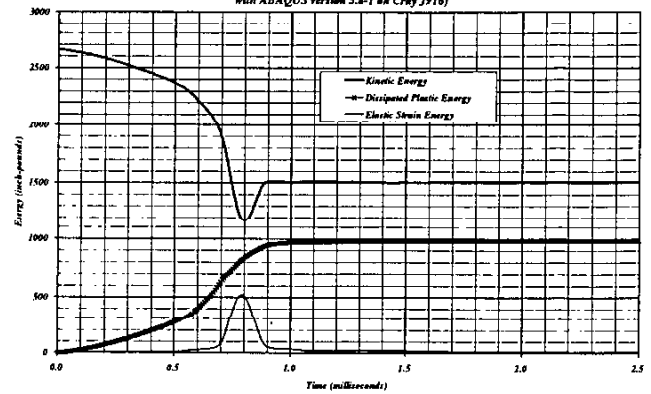


Figure 20. Time History of Kinetic, Plastic and Elastic Strain Energies during the 10-degree Inclined Upside Down Top Drop from 30-foot

Time History of Kinetic, Plastic and Elastic Strain Energies in the Bagless 3013 Can with a Steel Cylindrical Mass inside During the 20-degree Inclined Upside Down Top Drop from 30-foot (calculated with ABAQUS version 5.8.1 on Cray J916)

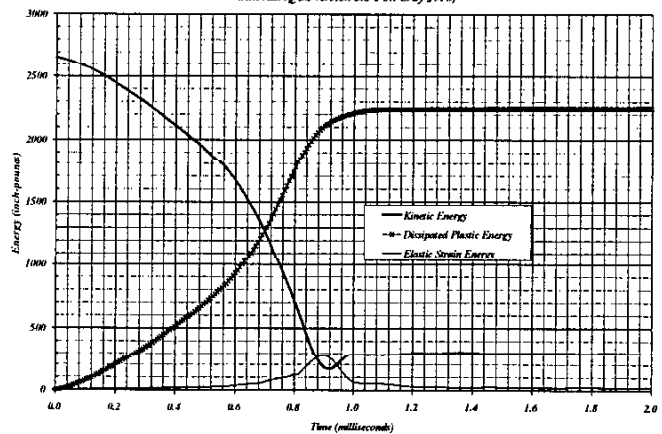


Figure 21. Time History of Kinetic, Plastic and Elastic Strain Energies during the 20-degree Inclined Upside Down Top Drop from 30-foot

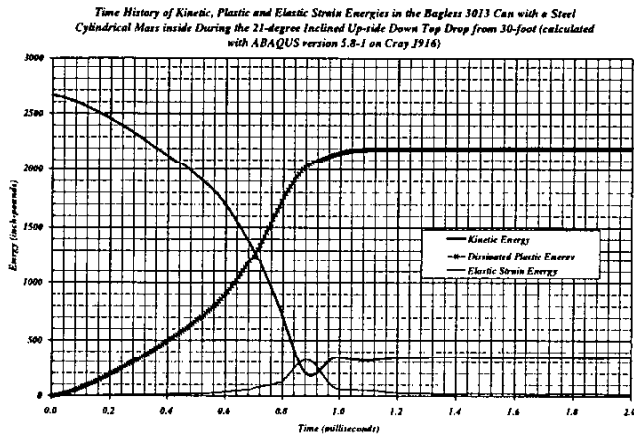


Figure 22. Time History of Kinetic, Plastic and Elastic Strain Energies during the 21-degree Inclined Upside Down Top Drop from 30-foot

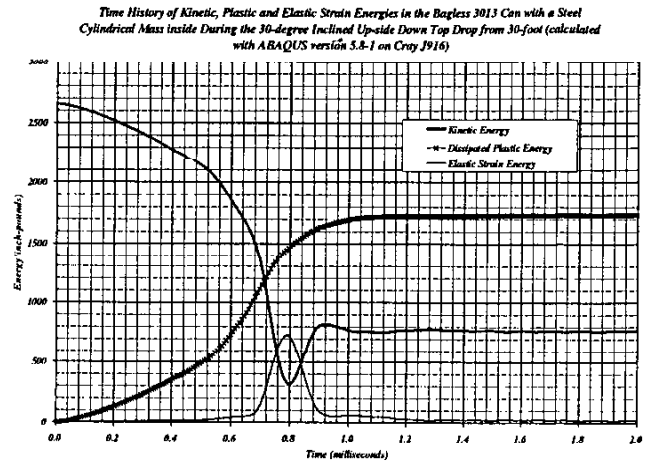


Figure 24. Time History of Kinetic, Plastic and Elastic Strain Energies during the 30-degree Inclined Upside Down Top Drop from 30-foot

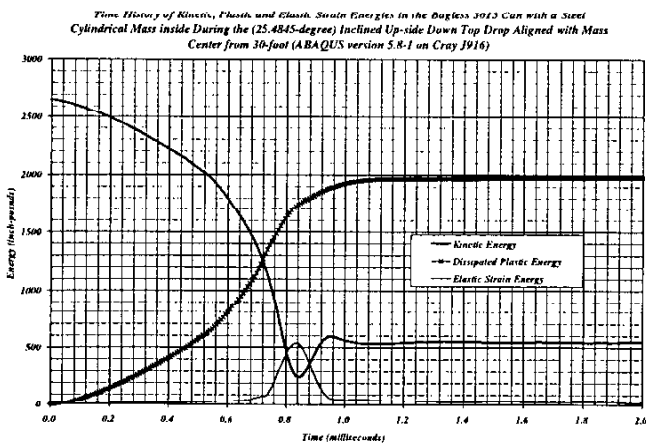


Figure 23. Time History of Kinetic, Plastic and Elastic Strain Energies during the 25.4845-degree Inclined Upside Down Top Drop Aligned with Mass Center from 30-foot

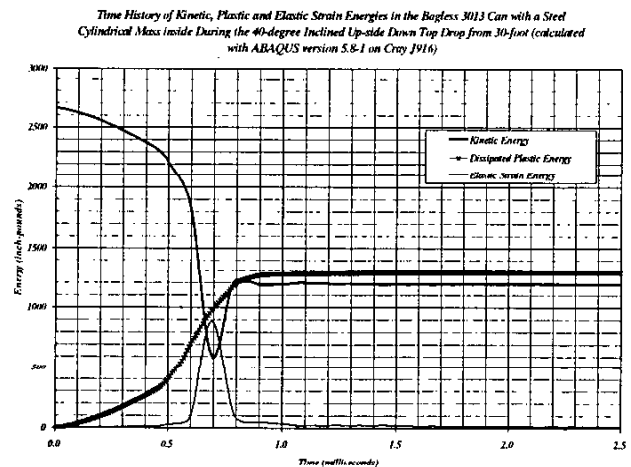


Figure 25. Time History of Kinetic, Plastic and Elastic Strain Energies during the 40-degree Inclined Upside Down Top Drop from 30-foot

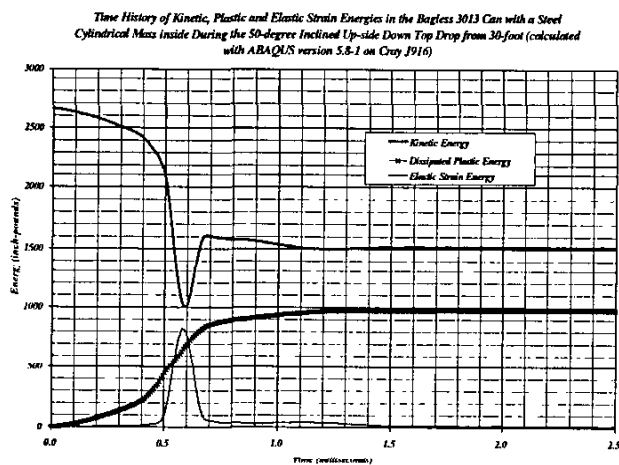


Figure 26. Time History of Kinetic, Plastic and Elastic Strain Energies during the 50-degree Inclined Upside Down Top Drop from 30-foot

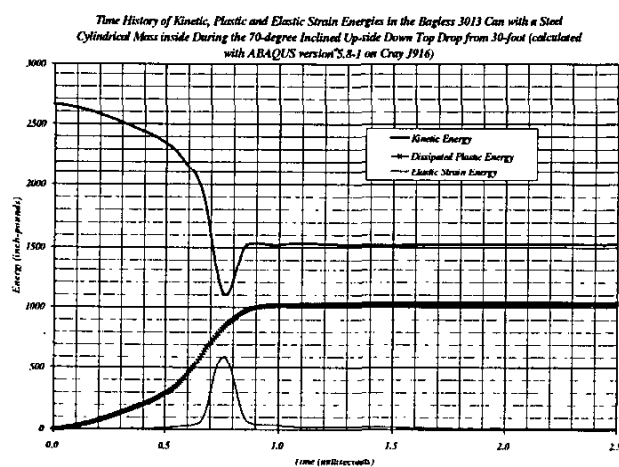


Figure 28. Time History of Kinetic, Plastic and Elastic Strain Energies during the 70-degree Inclined Upside Down Top Drop from 30-foot

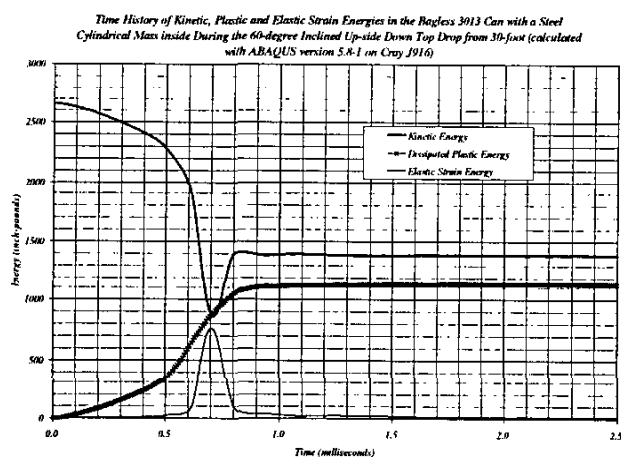


Figure 27. Time History of Kinetic, Plastic and Elastic Strain Energies during the 60-degree Inclined Upside Down Top Drop from 30-foot

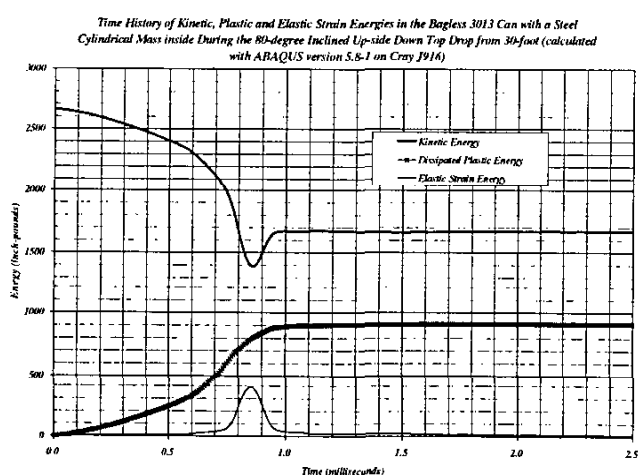


Figure 29. Time History of Kinetic, Plastic and Elastic Strain Energies during the 80-degree Inclined Upside Down Top Drop from 30-foot

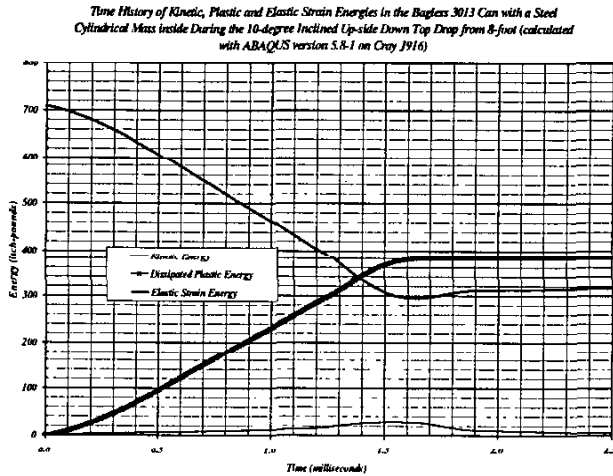


Figure 30. Time History of Kinetic, Plastic and Elastic Strain Energies during the 10-degree Inclined Upside Down Top Drop from 8-foot

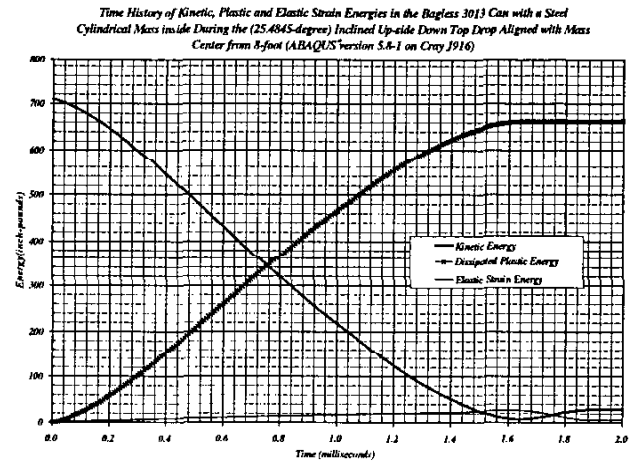


Figure 32. Time History of Kinetic, Plastic and Elastic Strain Energies during the 25.4845-degree Inclined Upside Down Top Drop Aligned with Mass Center from 8-foot

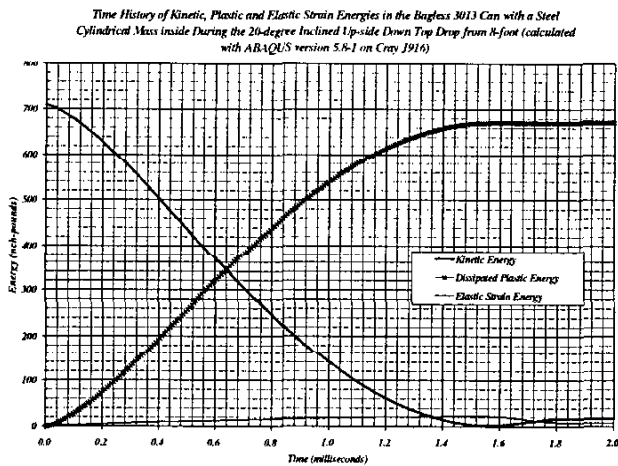


Figure 31. Time History of Kinetic, Plastic and Elastic Strain Energies during the 20-degree Inclined Upside Down Top Drop from 8-foot

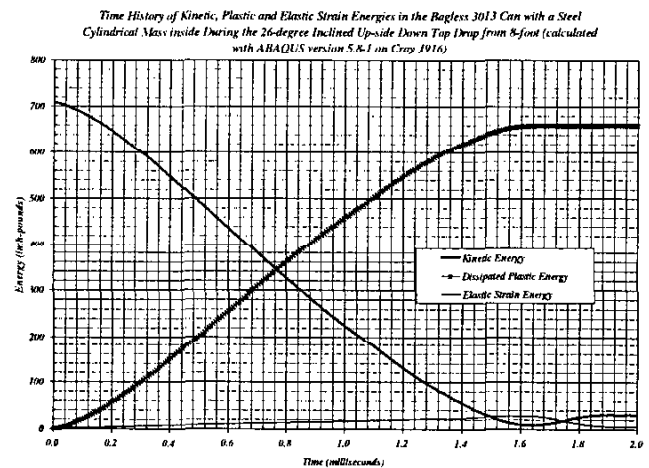


Figure 33. Time History of Kinetic, Plastic and Elastic Strain Energies during the 26-degree Inclined Upside Down Top Drop from 8-foot

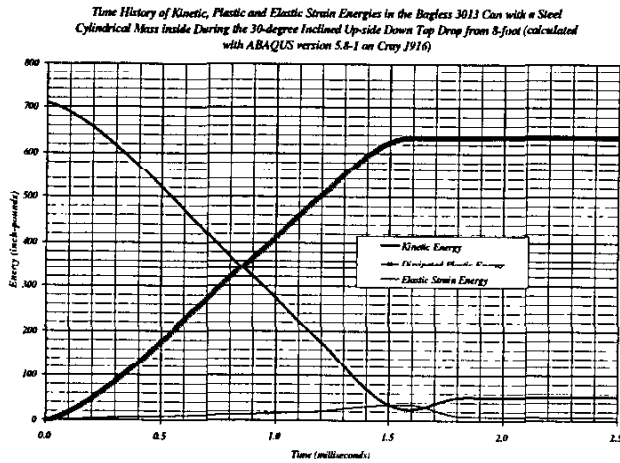


Figure 34. Time History of Kinetic, Plastic and Elastic Strain Energies during the 30-degree Inclined Upside Down Top Drop from 8-foot

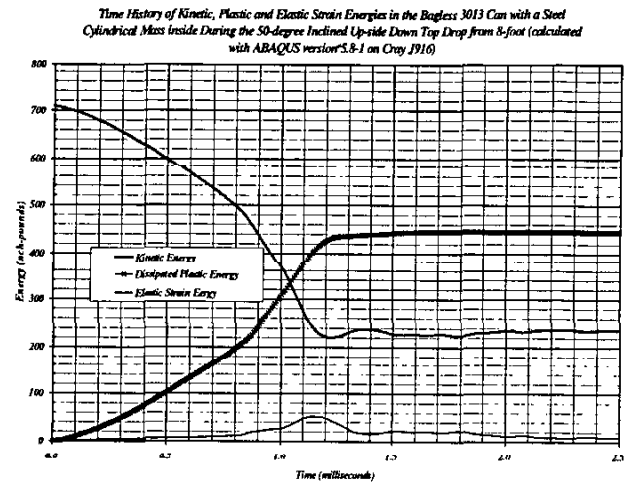


Figure 36. Time History of Kinetic, Plastic and Elastic Strain Energies during the 50-degree Inclined Upside Down Top Drop from 8-foot

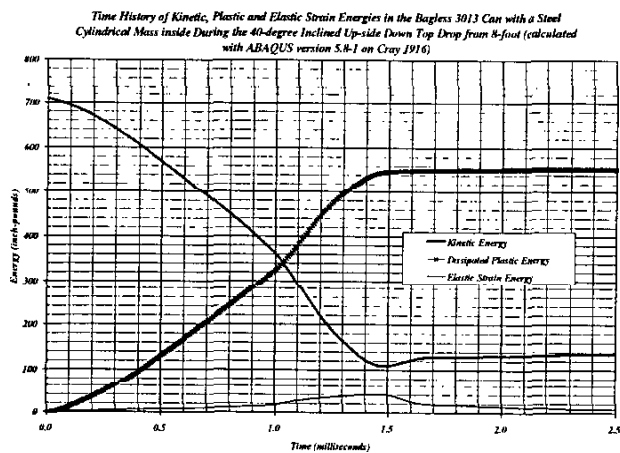


Figure 35. Time History of Kinetic, Plastic and Elastic Strain Energies during the 40-degree Inclined Upside Down Top Drop from 8-foot

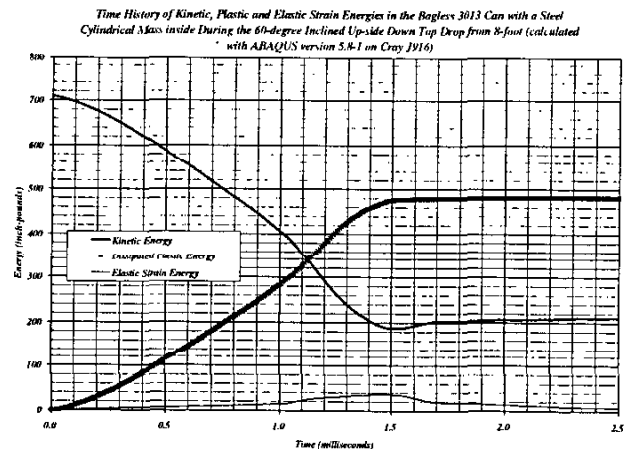


Figure 37. Time History of Kinetic, Plastic and Elastic Strain Energies during the 60-degree Inclined Upside Down Top Drop from 8-foot

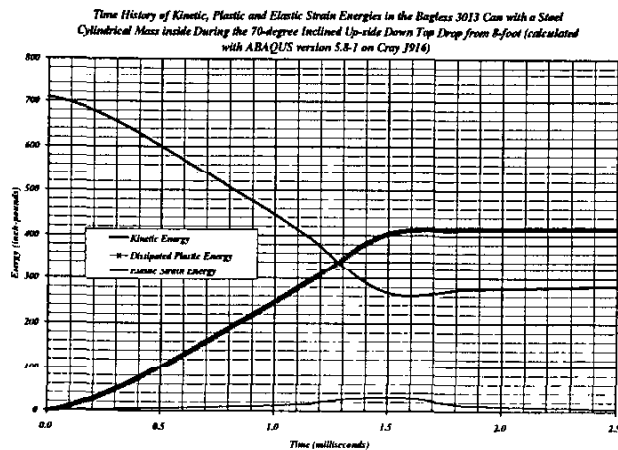


Figure 38. Time History of Kinetic, Plastic and Elastic Strain Energies during the 70-degree Inclined Upside Down Top Drop from 8-foot

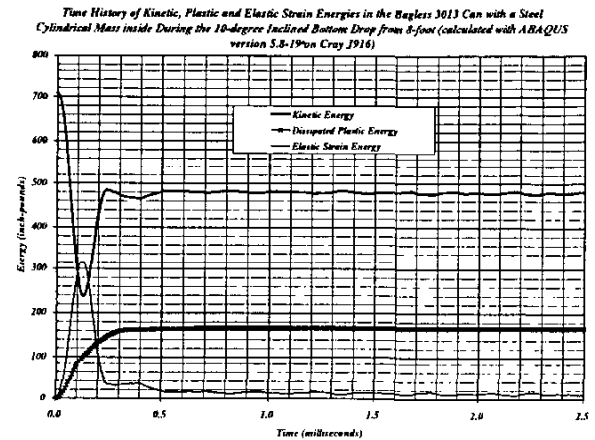


Figure 40. Time History of Kinetic, Plastic and Elastic Strain Energies during the 10-degree Inclined Bottom Drop from 8-foot

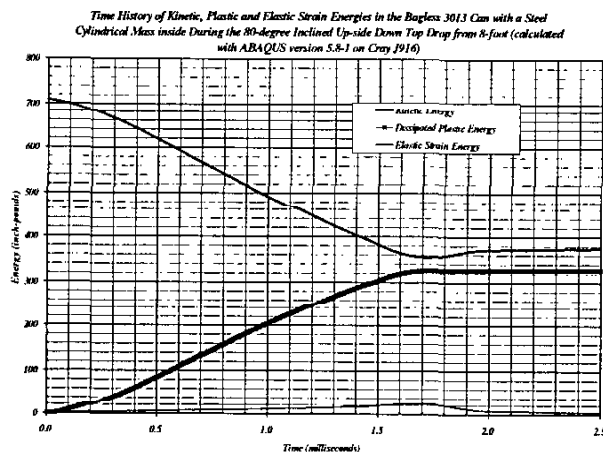


Figure 39. Time History of Kinetic, Plastic and Elastic Strain Energies during the 80-degree Inclined Upside Down Top Drop from 8-foot

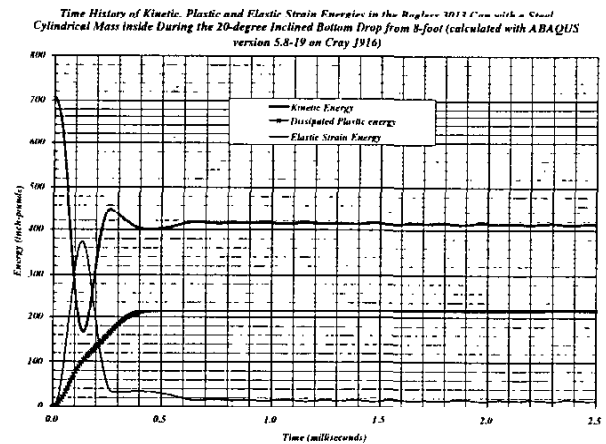


Figure 41. Time History of Kinetic, Plastic and Elastic Strain Energies during the 20-degree Inclined Bottom Drop from 8-foot

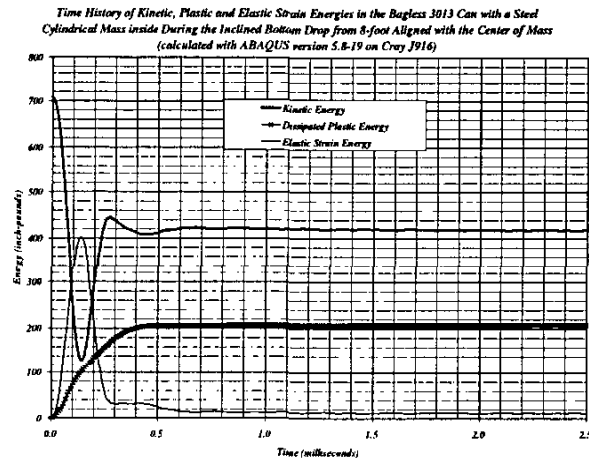


Figure 42. Time History of Kinetic, Plastic and Elastic Strain Energies during the 25.4845-degree Inclined Bottom Drop Aligned with Mass Center from 8-foot

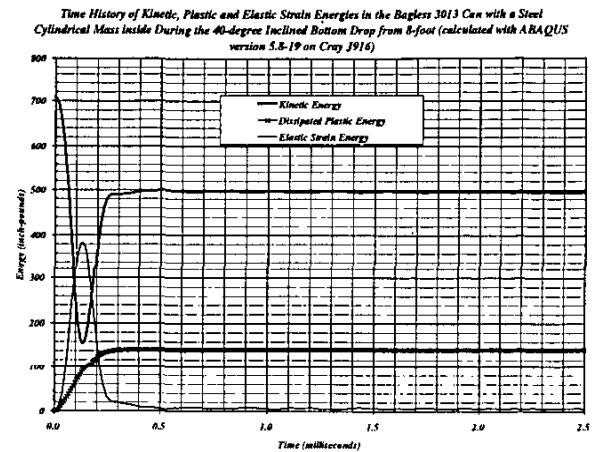


Figure 44. Time History of Kinetic, Plastic and Elastic Strain Energies during the 40-degree Inclined Bottom Drop from 8-foot

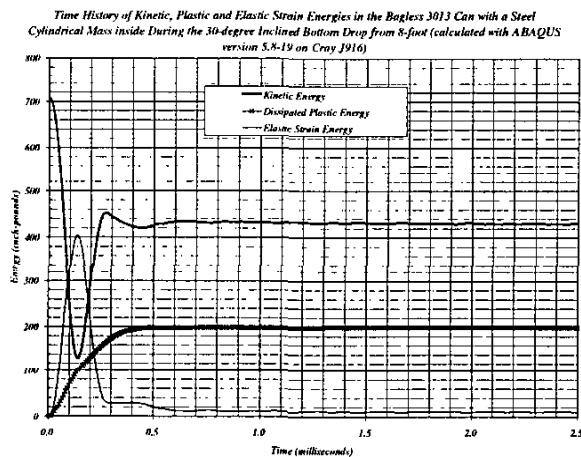


Figure 43. Time History of Kinetic, Plastic and Elastic Strain Energies during the 30-degree Inclined Bottom Drop from 8-foot

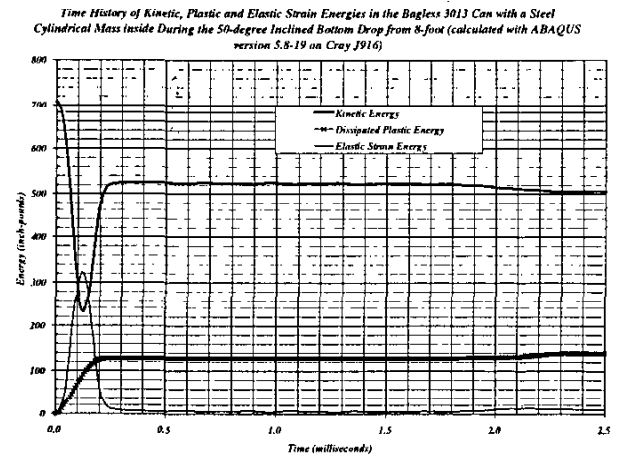


Figure 45. Time History of Kinetic, Plastic and Elastic Strain Energies during the 50-degree Inclined Bottom Drop from 8-foot

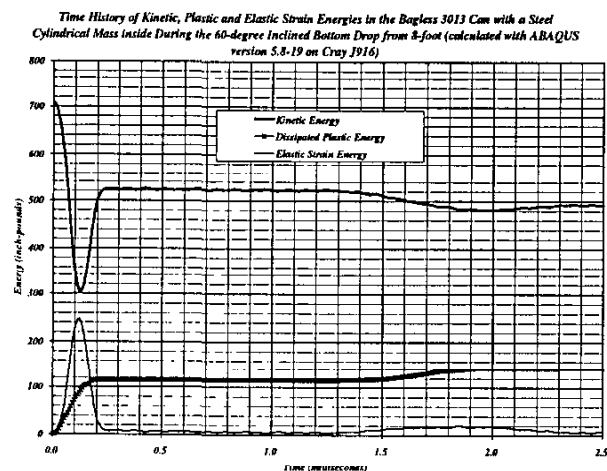


Figure 46. Time History of Kinetic, Plastic and Elastic Strain Energies during the 60-degree Inclined Bottom Drop from 8-foot

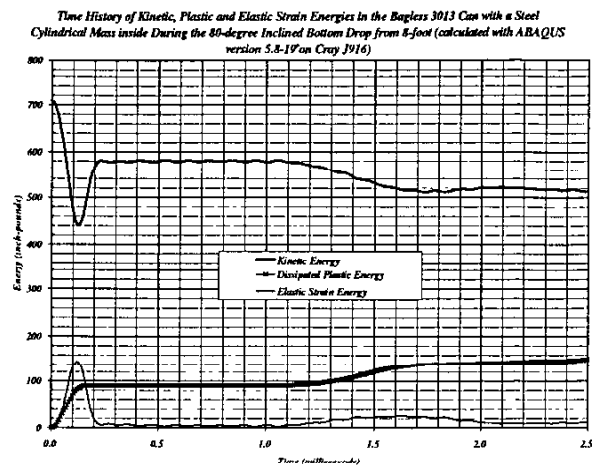


Figure 48. Time History of Kinetic, Plastic and Elastic Strain Energies during the 80-degree Inclined Bottom Drop from 8-foot

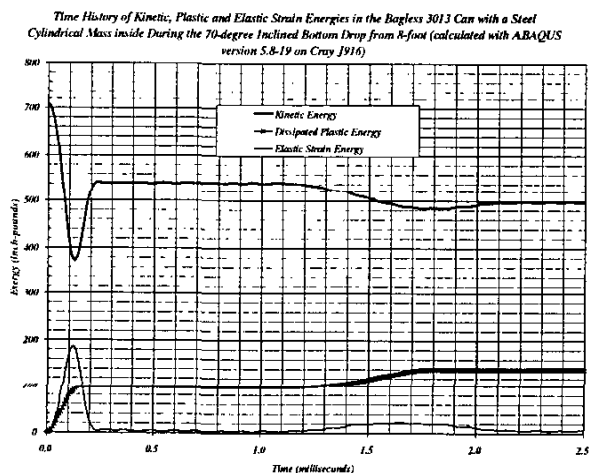


Figure 47. Time History of Kinetic, Plastic and Elastic Strain Energies during the 70-degree Inclined Bottom Drop from 8-foot

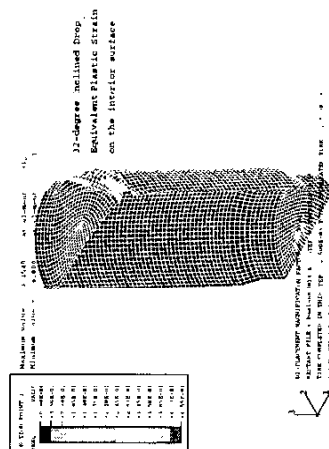


Figure 49. Contour Plot of Equivalent Plastic Strain in the Vessel with Uniformly Distributed Mass at the End of 32-degree Inclined Upside Down 30-foot Drop

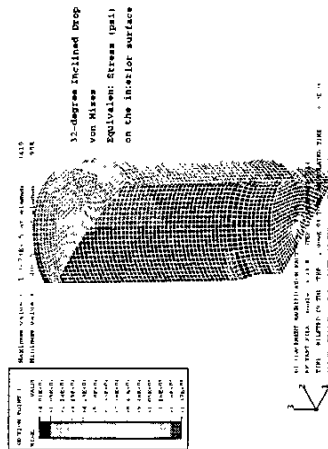


Figure 50. Contour Plot of von Mises Equivalent Stress in the Vessel with Uniformly Distributed Mass at the End of 32-degree Inclined Upside Down 30-foot Drop

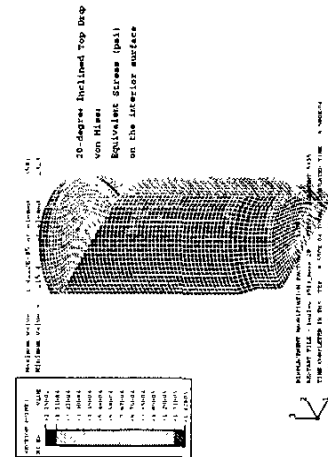


Figure 52. Contour Plot of von Mises Equivalent Stress in the Vessel with Steel Cylindrical Mass at the End of 20-degree Inclined Upside Down 30-foot Drop

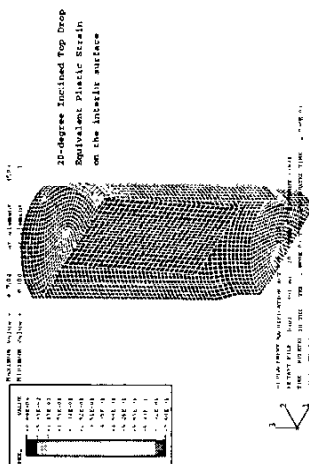


Figure 51. Contour Plot of Equivalent Plastic Strain in the Vessel with Steel Cylindrical Mass at the End of 20-degree Inclined Upside Down 30-foot Drop

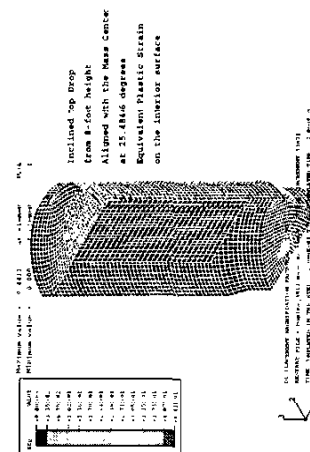


Figure 53. Contour Plot of Equivalent Plastic Strain in the Vessel with Steel Cylindrical Mass at the End of 25.4845-degree Inclined Upside Down 8-foot Drop

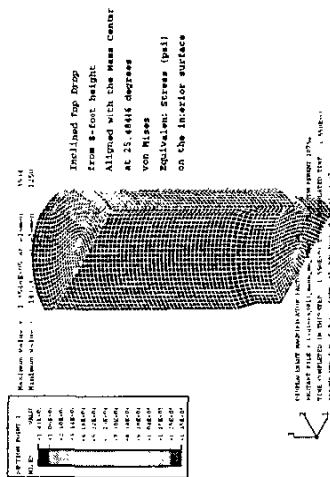


Figure 54. Contour Plot of von Mises Equivalent Stress in the Vessel with Steel Cylindrical Mass at the End of 25.4845-degree Inclined Upside Down 8-foot Drop

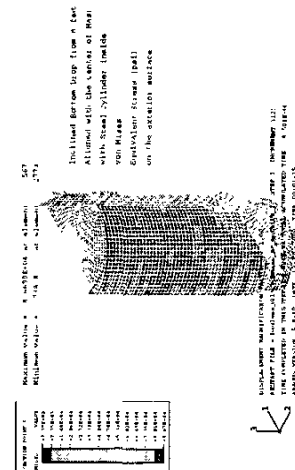


Figure 56. Contour Plot of von Mises Equivalent Stress in the Vessel with Steel Cylindrical Mass at the End of 27.8177-degree Inclined Bottom 8-foot Drop.

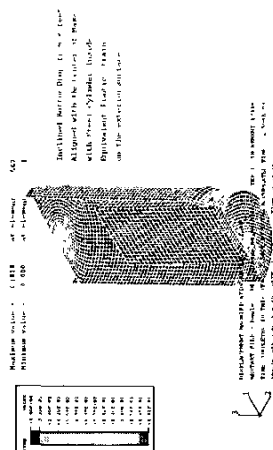


Figure 55. Contour Plot of Equivalent Plastic Strain in the Vessel with Steel Cylindrical Mass at the End of 27.8177-degree Inclined Bottom 8-foot Drop